Supplementary Figures

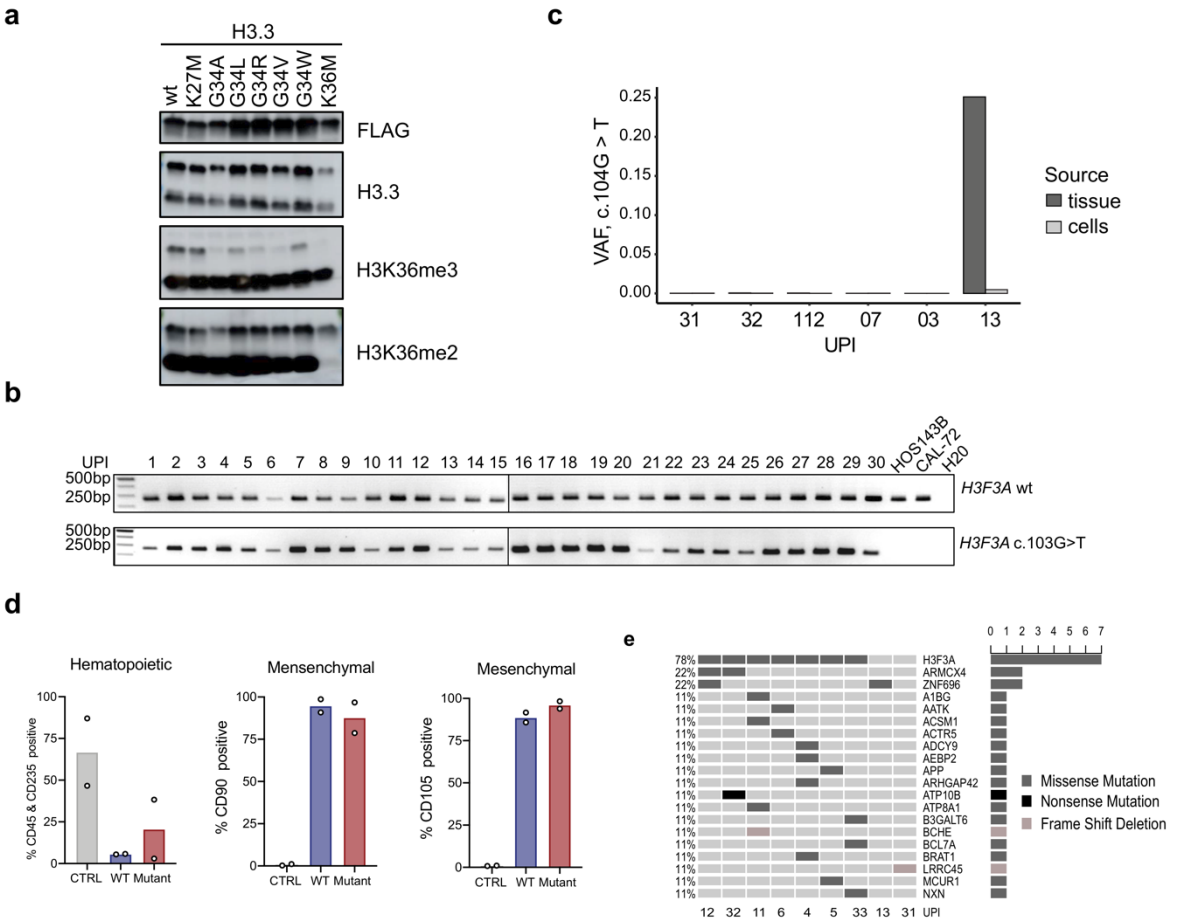

Figure S1: Initial characterization of GCTB samples.

a. Western blots of whole cell lysates obtained from HEK293T cells stably expressing H3.3-HA-3XFLAG wildtype or respective mutants as indicated. **b**. Top: PCR for wild-type *H3F3A* allele as control; bottom: mutation-specific PCR of the heterozygous *H3F3A* c.103G>T mutation in bulk DNA isolated from GCTB tumor resections. Osteosarcoma cell lines HOS143B and CAL-72 were used as negative controls. PCR assay cannot discriminate between c103G>T (G34W) and c103GG>TT (G34L) mutations. Vertical bar separates two independent gels. **c**. Quantification of the mutation at position 104 in the *H3F3A* gene (c.143G>T) leading to the H3.3 G34L substitution in tumor resections and derived stromal cell lines using deep targeted resequencing. VAF, variant allele frequency. **d**. FACS analysis with CD45, CD235, CD90 and CD105 specific antibodies of two H3.3 WT and two H3.3 MUT stromal cell lines (UPI: 13, 34, 20 und 21) in comparison to human bone marrow. **e**. Most abundant single nucleotide variants (SNV) with driver potential based on whole-genome sequencing (WGS) of nine patient-derived cell lines.

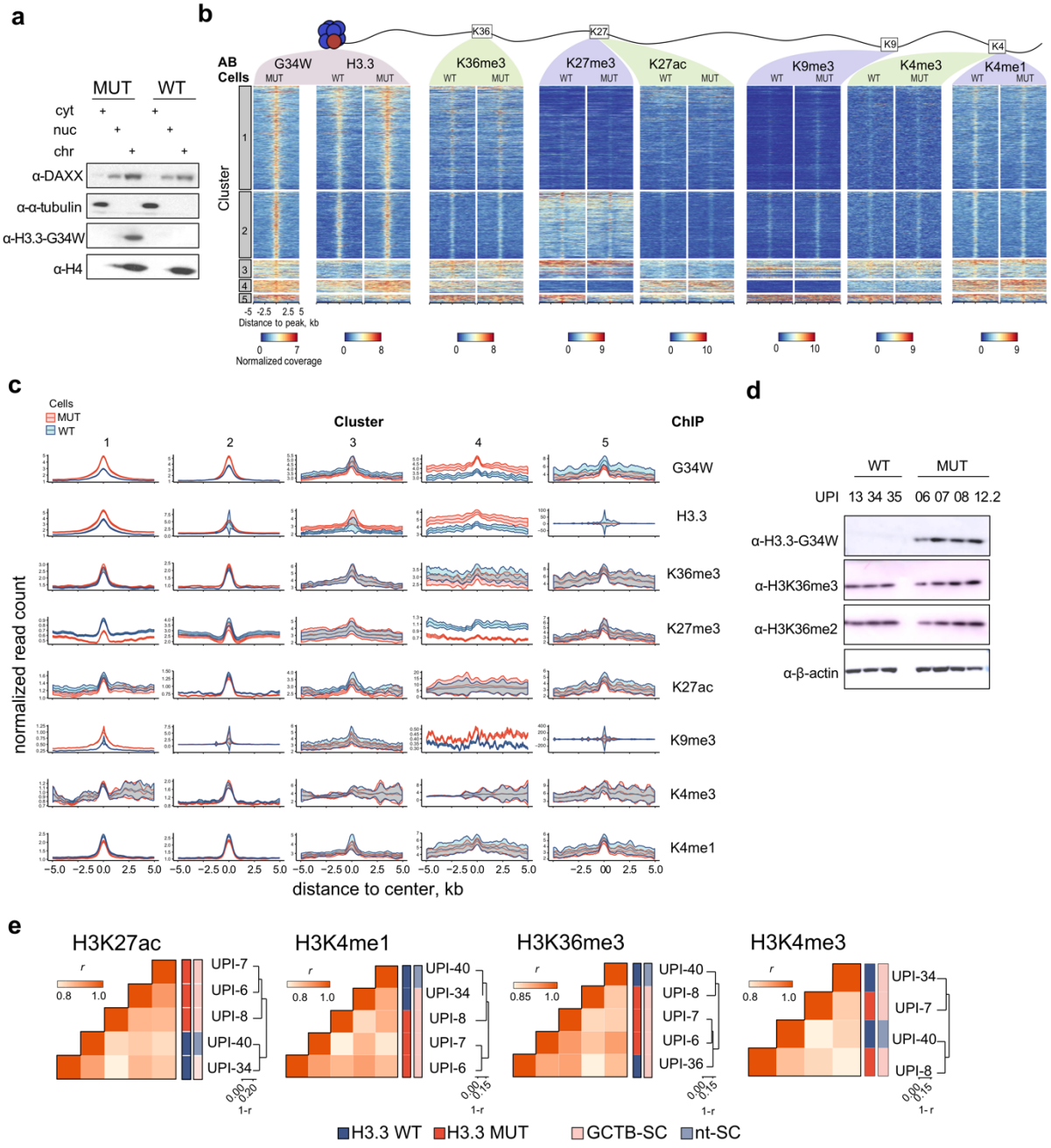

Figure S2: Global epigenetic alterations in H3.3 MUT stromal cells

a. Western blot analysis of fractionated protein from two GCTB stromal cells (unified patient identifiers, UPI-6 and UPI-13); either positive (+; H3.3 MUT) or negative (-; H3.3 WT) for H3.3-G34W, using antibodies against α-tubulin, H3.3-G34W, H4 and DAXX. Cyt, cytosol; Nuc, nucleus; Chr, chromatin. **b.** Genomic summary heatmap of ChIP-seq signals of H3.3-G34W, wild type H3.3 and histone marks at H3.3-G34W incorporation regions. Each row corresponds to one of the H3.3-G34W enriched loci. Clusters were obtained using *k*-means clustering in a space spanned by the columns of the displayed heatmap. **c**. Alterations of chromatin accessibility (ATAC) and histone marks (H3K4me1, H3K4me3, H3K27ac, H3K27me3, H3K36me3 and H3K9me3) around H3.3-G34W sites. Solid lines represent the mean profiles while ribbons show standard errors of the mean across all summarized regions. Cluster numbers correspond to those given in **b**. **d**. Western blot analysis of global levels of H3K36 methylation in whole cell lysates of H3.3 WT and H3.3 MUT stromal cells. UPI-12.2 represents a relapse case. **e**. Hierarchical clustering with correlation distance of H3K27ac,

H3K4me1, H3K36me3 and H3K4me3 profiles in H3.3 WT (blue) and H3.3 MUT (red) cells. Heatmaps represent pairwise Pearson correlation coefficients (*r*) between respective modification profiles of two cell lines. Dendrograms were obtained with agglomerative hierarchical clustering with 1-r distance and average linkage. Heatmap color codes represent *H3F3A* mutational status (inner), and the cell type (outer), the common legend for all heatmaps is given at the bottom. nt-SC, nontumoral stromal cells; UPI, unified patient identifier.

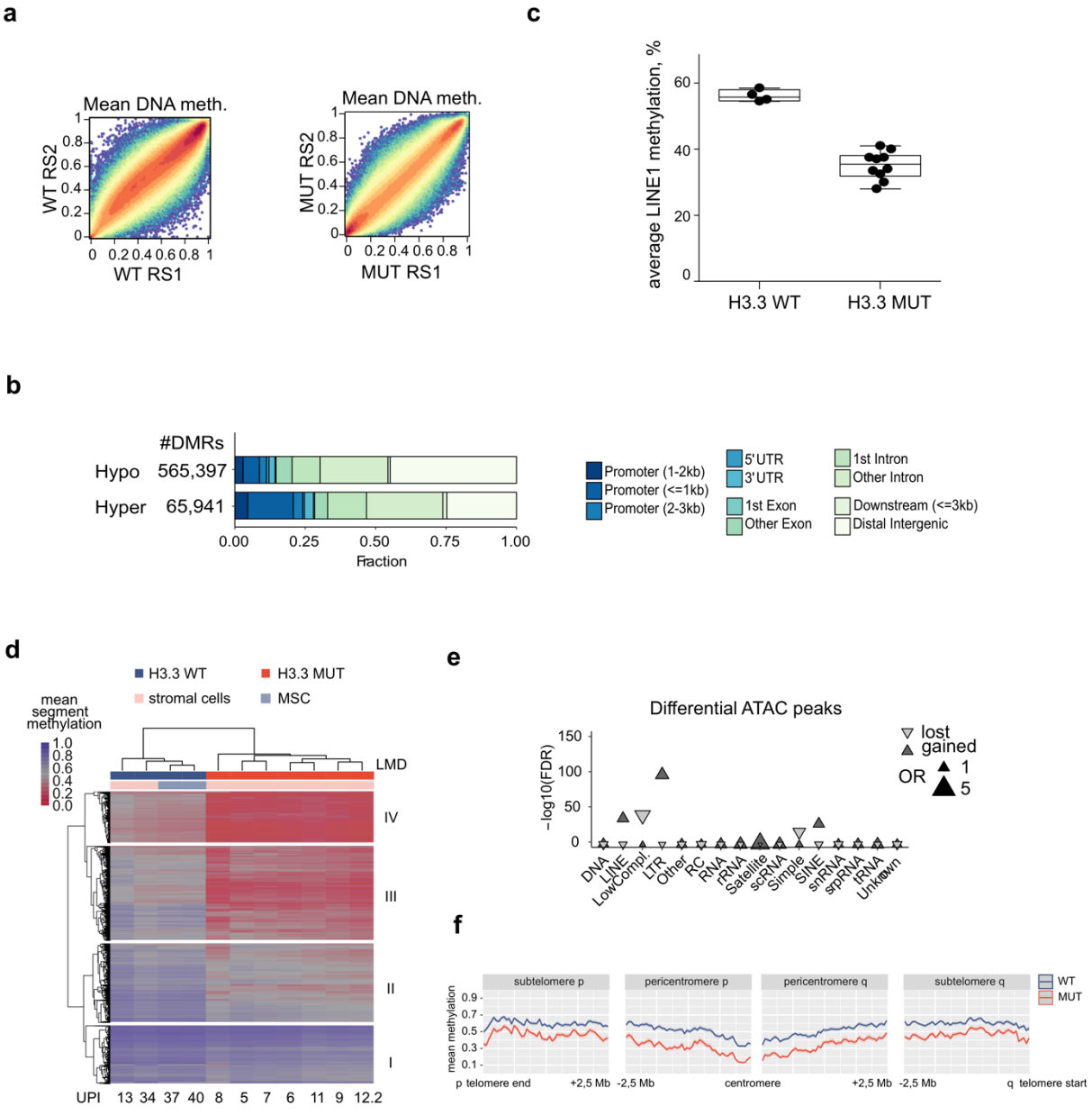

Figure S3: Heterochromatin defects in H3.3 MUT stromal cells

a. Binned scatterplot of intra-group genome wide DNA methylation profiles from WGBS in H3.3 WT cells (top) and H3.3 MUT cells (bottom). Each group was split into two random subsets and average profiles of the subsets were used to generate the binned scatterplots. RS1 and RS2, random sample subsets 1 and 2, respectively. Hexagon color represents binned density gradient of 1 (blue), 1000 (yellow) and 10^6 (red) points. **b**. Genomic distribution of differentially methylated regions (DMR) between H3.3 WT and H3.3 MUT cells with respect to gene model annotation. Hyper, DMRs hypermethylated in H3.3 MUT; Hypo, DMRs hypomethylated in H3.3 MUT. **c**. Quantification of average DNA methylation levels at LINE1 elements using MassARRAY in H3.3 WT and H3.3 MUT cells. Points represent individual patients, central line represents the mean, box covers the inter-quartile range, whiskers extend from minimal to maximal values. Difference is significant ($p<10^{-3}$, two-sample t-test). **d**. Mean methylation levels of segments falling into one of the four major large methylation domains (LMD). Dendrograms over columns and rows show clustering of samples using agglomerative hierarchical clustering with Euclidean distance and average linkage. GCTB-SC, GCTB-derived

stromal cells; nt-SC, nontumoral stromal cells. **e.** Genomic overlap analysis of differential ATAC peaks with repetitive elements. “Lost” and “gained” refer to peaks showing a decrease (disappearance) or increase (emergence) in H3.3 MUT, respectively. FDR, false discovery rate; OR, odds ratio. **f**. Mean DNA methylation profiles of subtelomeric and pericentromeric regions in H3.3 WT and H3.3 MUT cells.

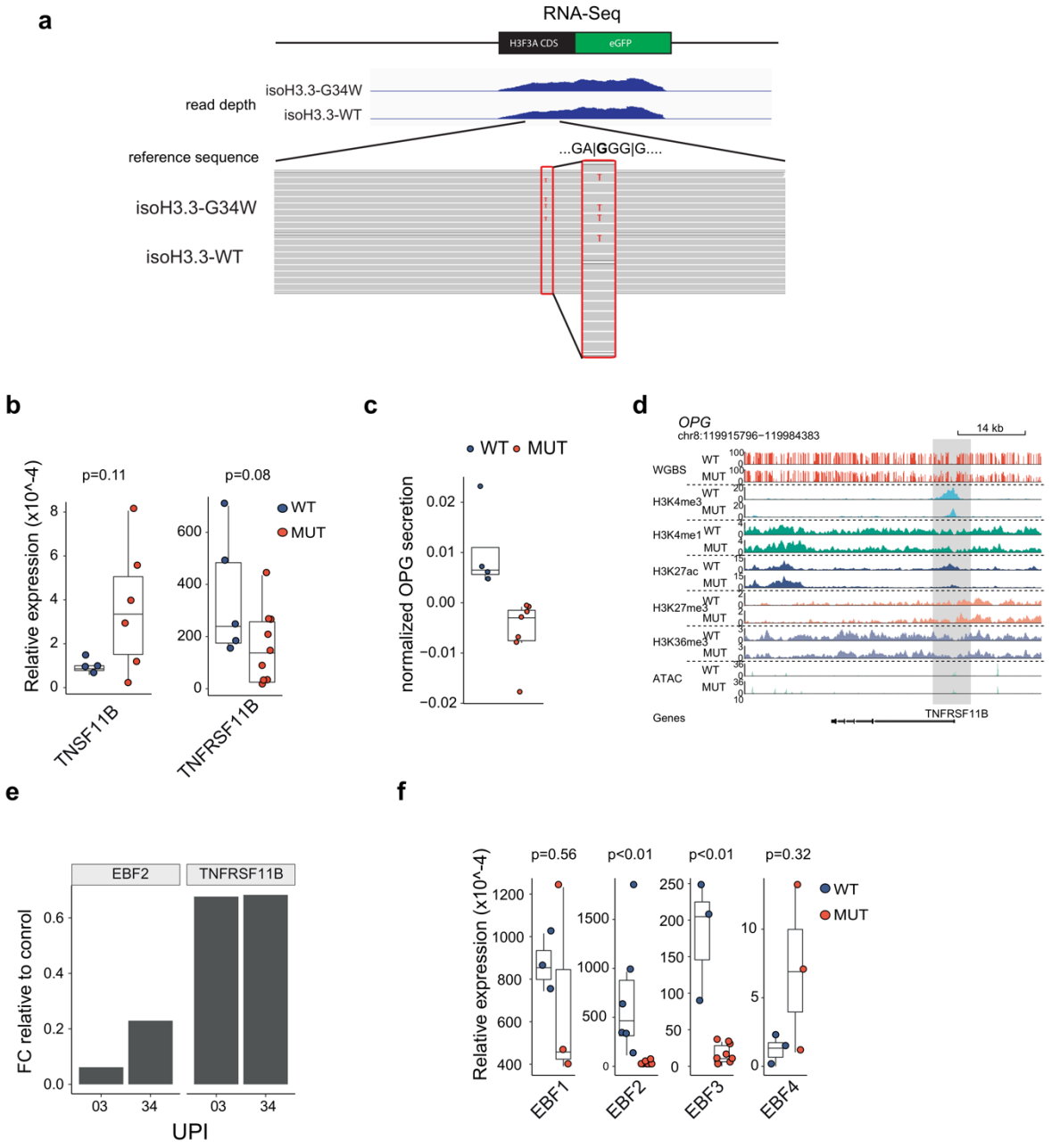

Figure S4: Isogenic H3.3 G34W HeLa cells and the osteolytic phenotype of GCTB

a. Genomic browser view of RNA-Seq data for *H3F3A* in iso-H3.3-G34W and iso-H3.3-WT HeLa cells showing the locus-endogenous knock-in of the G34W-mutation. IGV snapshot of the coverage depth and single-read display is made based on an alignment to the reference sequence of the full construct. **b**. Expression levels of OPG (*TNFRSF11B*) and RANKL (*TNFS11*) in H3.3 WT and H3.3 MUT cells analyzed with qRT-PCR**.** Expression is shown relative to *GAPDH*. **c.** OPG ELISA with cell culture supernatant of H3.3 WT and H3.3 MUT cells. Amount of secreted OPG is shown normalized to cell viability as a surrogate for cell number measured by cell titer blue assay. Observations were centered per replicate and averaged for each patient. Each dot represents a different patient. Boxplot bar represents mean, box gives the IQR, whiskers span additional 1.5*IQR below and above the bars. Unpaired t-test p=0.075. **d**. Genomic browser view of the OPG encoding gene *TNFRSF11B*. Each lane (dash-separated) represents normalized averaged signals of DNA methylation, the level of

H3K4me3, H3K4me, H3K9me3, H3K27ac, H3K27me3, H3K36me3 and ATAC in several replicates of H3.3 WT (lane-wise top) or H3.3 MUT (lane-wise bottom) cells. **e.** Expression analysis of EBF2 and OPG (*TNFRSF11B*) by qPCR 48 hours after siRNA mediated knockdown of EBF2 in two H3.3 WT cell lines (UPI-03, UPI-34). Fold change (FC) relative to expression in cells transfected with a control siRNA. **f**. Expression levels of all members of the EBF family in H3.3 WT and H3.3 MUT cells analyzed with qRT-PCR**.** Expression is shown relative to *GAPDH.*

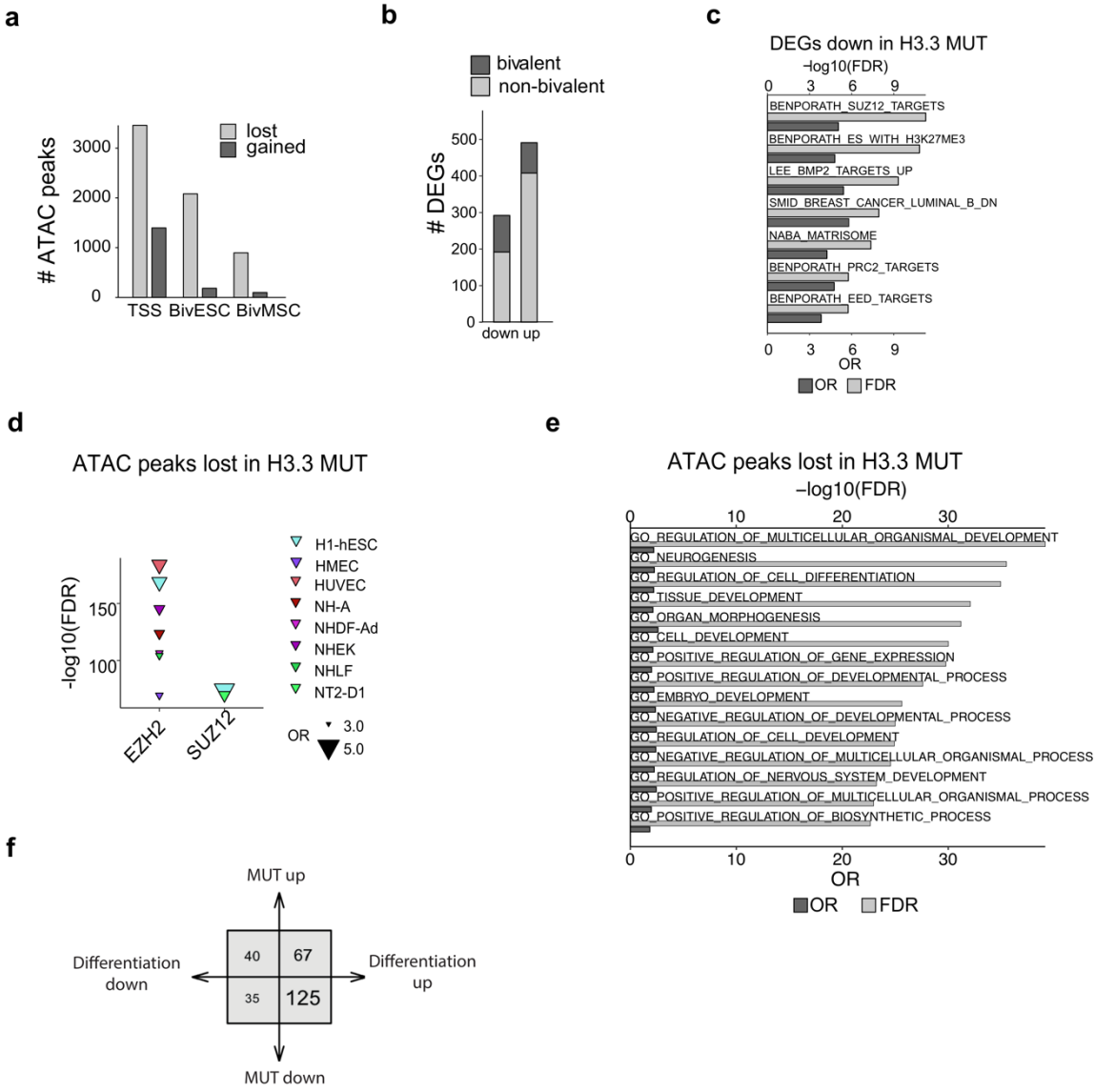

Figure S5: Osteogenic differentiation of H3.3 MUT stromal cells

a. Enrichment of differentially accessible chromatin sites at transcription start sites (TSS) of bivalent genes. Bars represent numbers of differential ATAC peaks with increased (gain) and decreased (loss) signal in H3.3 MUT cells overlapping bivalent TSSs. TSS, all Ensemble TSS; BivESC, consensus human bivalent TSS in ESC as defined in Court et al (Ref. 65 in the main text); BivMSC, bivalent TSS defined in nt-SC cells using peak overlaps. **b**. Fraction of bivalent genes in the total set of differentially expressed genes (DEG)**. c.** Top significantly enriched gene sets from the MSigDB collection of curated gene sets (C2) obtained with overrepresentation analysis of DEGs downregulated in H3.3 MUT. OR, odds ratio; FDR, false discovery rate. **d**. Genomic overlap enrichment analysis of differential ATAC peaks lost in H3.3 MUT with TFBS (ENCODE). Symbol color labels various cell types as they appear in the *LOLA* core database. ESC, embryonic stem cell; HUVEC, human umbilical vein endothelial cells; LC, leukemia cell; OR, odds ratio. **e**. Top significantly enriched gene sets from the MSigDB collection of Gene Ontology gene sets (C5) obtained with overrepresentation analysis of genes containing one or more differential ATAC-seq peaks lost in H3.3 MUT within 10kb from a canonical TSS from Ensemble. OR, odds ratio; FDR, false discovery rate. **f**. Overlap of DEGs between H3.3 WT and H3.3 MUT stromal cells and genes significantly altered during osteogenic differentiation.